

LETTER | MARCH 03 2025

Ion cyclotron range of frequencies plasma production and heating in the large helical device

V. E. Moiseenko ; Yu. V. Kovtun ; H. Kasahara ; T. Seki ; K. Saito ; R. Seki ; S. Kamio ; A. Dinklage ; D. Hartmann ; H. Laqua ; T. Stange ; S. Lazerson ; A. Alonso ; T. Wauters ; Ye. O. Kazakov ; J. Ongena ; I. E. Garkusha 



Phys. Plasmas 32, 030701 (2025)

<https://doi.org/10.1063/5.0248769>



Articles You May Be Interested In

ICRF production of plasma with hydrogen minority in Uragan-2M stellarator by two-strap antenna

Phys. Plasmas (April 2024)

RF Plasma Production in Uragan-2M Torsatron

AIP Conference Proceedings (September 2007)

Dual-polarization single-chord plasma interferometry in stellarators/torsatrons

Rev. Sci. Instrum. (September 2020)



Physics of Plasmas

Special Topics Open
for Submissions

[Learn More](#)

Ion cyclotron range of frequencies plasma production and heating in the large helical device

Cite as: Phys. Plasmas **32**, 030701 (2025); doi: 10.1063/5.0248769

Submitted: 13 November 2024 · Accepted: 15 February 2025 ·

Published Online: 3 March 2025



View Online



Export Citation



CrossMark

V. E. Moiseenko,^{1,2} Yu. V. Kovtun,^{1,a)} H. Kasahara,³ T. Seki,³ K. Saito,⁴ R. Seki,³ S. Kamio,⁵ A. Dinklage,⁶ D. Hartmann,⁶ H. Laqua,⁶ T. Stange,⁶ S. Lazerson,⁶ A. Alonso,⁷ T. Wauters,⁴ Ye. O. Kazakov,⁸ J. Ongena,⁸ and I. E. Garkusha^{1,9}

AFFILIATIONS

¹Institute of Plasma Physics of the National Science Center, Kharkiv Institute of Physics and Technology, 1, Akademichna St., 61108 Kharkiv, Ukraine

²Ångström Laboratory, Uppsala University, 75104 Uppsala, Sweden

³National Institute for Fusion Science, 322-6 Oroshi-cho, Toki, Japan

⁴ITER Organization, Route de Vinon-sur-Verdon, CS 90046, 13067 St. Paul Lez Durance Cedex, France

⁵University of California Irvine, Irvine, California 92697, USA

⁶Max-Planck-Institut für Plasmaphysik, Wendelsteinstraße 1, 17491 Greifswald, Germany

⁷Laboratorio Nacional de Fusion, CIEMAT, Complutense, 40, 28040 Madrid, Spain

⁸Laboratory for Plasma Physics, ERM/KMS, TEC Partner, 30, Avenue de la Renaissancelaan, 1000 Brussels, Belgium

⁹V.N. Karazin Kharkiv National University, 4 Svobody Sq., 61022 Kharkiv, Ukraine

^{a)} Author to whom correspondence should be addressed: kovtun41@gmail.com

ABSTRACT

Plasma production in stellarators with ion cyclotron heating is complementary to the widely used electron cyclotron heating (ECRH). The prospective light ion minority scenario developed and tried on Uragan-2M and Large Helical Device (LHD) stellarators had been reexamined at LHD. The distinctive feature of this attempt is that the parameters of plasma produced are better than before and are comparable with those of plasma produced by the ECRH. This new possibility of ion cyclotron heating, if it becomes practical, motivates rethinking of the role of ion cyclotron heating in stellarator machines.

© 2025 Author(s). All article content, except where otherwise noted, is licensed under a Creative Commons Attribution (CC BY) license (<https://creativecommons.org/licenses/by/4.0/>). <https://doi.org/10.1063/5.0248769>

Plasmas in stellarators are created by radio frequency (RF) waves in the range of ion cyclotron frequencies (ICRF).¹ Earlier experiments on both plasma break-down and heating plasma exclusively by RF methods were carried out mainly on small stellarators. Reports from the Compact Helical System (CHS),² Wendelstein 7-AS,³ Uragan-3M (U-3M) and Uragan-2M (U-2M),^{4,5} and H-1⁶ definitively demonstrate the possibility of producing plasma with a density of 10^{18} – 10^{19} m⁻³ using RF discharges only. However, the resulting electron temperatures were found to be quite low, ranging from some eV to some hundreds of eV. In addition to the aforementioned devices, experiments on the production of RF plasma have also been carried out in the Large Helical Device (LHD). Using a folded waveguide antenna, a density of 3.0×10^{18} m⁻³ was achieved, and the electron temperature in the center was roughly several tens of eV.⁷ Extending these findings to large

stellarators indicates that standard RF equipment must be made more complex to fit the aforementioned scenarios. To this end, LHD experiments demonstrate that machine size must be taken into account, and efforts must increase accordingly. In contrast, electron cyclotron heating (ECRH) at the second harmonic extraordinary mode (X2 regime) robustly creates and heats plasmas, making it a compelling argument for its wide usage.

From a technical point of view, ICRF plasma production is of interest for stellarators only if it focuses on using the ICRF heating equipment. The scenario that meets this requirement is documented in Ref. 8, in which the plasma was made of a gas mixture containing hydrogen. As with all scenarios, it should couple RF power to the electrons in a wide plasma density range, from very low at the initial stage to high at the final stage (see also Ref. 9). At low plasma densities, the

direct slow-wave excitation by the antenna is necessary to heat the plasma electrons. Strap antennas, widely used for ICRF, however, are designed for fast wave excitation. Beneficial for an efficient plasma break-down, the power needed to couple to the plasma is small, and parasitic slow-wave excitation by the antenna is, as a rule, sufficient for the initiation of plasma production.

At high plasma densities, the electron heating results from mode conversion,¹⁰ which is widely established for two-ion-plasmas. Experiments at U-2M^{8,11–15} have identified discharge conditions that allow for producing fully ionized ICRF plasma in stellarators. This particular scenario requires light minority ions, for which the ion cyclotron resonance zone resides in the plasma. In experiments with H₂ + He mixture in U-2M, relatively high density ($\sim 10^{19} \text{ m}^{-3}$) plasmas were produced, but, again, at low ion and electron temperatures.^{8,11–15}

Given the resulting motivation to develop reliable plasma startup scenarios, studies on LHD^{14,16–18} were conducted. As a starting point for our studies, ICRF plasma production was demonstrated using field-aligned antennas.¹⁶ The RF power was limited to 0.2 MW to avoid arcing on RF antennas that could result in detrimental impurity fluxes or even in RF system damage. In this way, low plasma density ($9.5 \times 10^{17} \text{ m}^{-3}$) was obtained, the antenna–plasma coupling was poor, and the produced plasmas were not fully ionized. In subsequent experiments, the injected RF power was significantly increased,^{14,17} resulting predictably in a sixfold increase in the plasma density up to $6 \times 10^{18} \text{ m}^{-3}$. Still, the electron temperature was low, and light impurities were not fully ionized, as indicated by the lack of recombination lines peaks after the RF pulse. Curiously, when the cold initial plasma is prepared by ECRH pulse, ion cyclotron resonance heating (ICRH) alone rises both electron and ion temperatures and, after this, sustains this hot plasma.¹⁷ Summarizing the findings, break-down and heating were not obtained within a discharge. Therefore, the goal of the studies is to demonstrate both the break-down and plasma heating employing the same RF set-up. In order to qualify the approach for larger devices, the scalability of this ICRF pre-ionization scenario is examined as well in LHD.

LHD is a superconducting, large-scale, heliotron-type device with a major plasma radius of $R_{\text{ax}} = 3.6 \text{ m}$ and a mean minor radius of $a_p = 0.6 \text{ m}$, resulting in a plasma volume of about 30 m^3 .¹⁹ In the reported experiments, the magnetic field was kept at 2.75 T on the magnetic axis. Then, at the used heating frequency of 38.5 MHz, the protium-cyclotron-resonance zone crosses the plasma column vertically. The ICRF heating system of LHD includes the hand-shake form (HAS) antenna²⁰ and the field-aligned-impedance-transforming (FAIT) antenna.²¹ Each antenna consists of two parts, upper (U) and lower (L), which can be fed independently. To avoid a strong voltage increase on the RF system elements, especially at the initial stage of plasma production at the beginning of the RF pulse, the RF power is gradually ramped up to the designated level. The ramping-up time is 0.1–0.2 s to arrive at moderate power levels of $\sim 250 \text{ kW}$. A comparable approach was realized at U-2M, where the RF power is increased step-wise.¹⁰ The idea of this approach is to create plasma at low power levels, thereby providing necessary antenna-plasma coupling for higher RF powers.

The crucial novelty of the approach reported here is the gas fueling scheme. We examine two ways of gas fueling, a continuous and a pulsed one. In the continuous mode, a gas mixture is created in the

LHD vacuum vessel by independent supply of hydrogen and helium. Hydrogen was injected through ports 3.5 and 5.5 l and helium through port 5.5 l.²² The flow rates were controlled by varying the voltage on the piezo-electric valves. The steady-state pressure and the concentration of hydrogen and helium were monitored by the vacuum gauges and mass spectrometer, respectively. In addition to the constant hydrogen and helium gas puff, a pre-programmed gas injection of helium was used in the pulsed mode. The 5.5 l port gas flow rate was varied and optimized during the shot. Experimentally selected such a regime at which a significant increase in plasma density after helium injection was observed. This effect, for example, had been achieved in five pulses of helium injection with a duration of 4 ms of each pulse at maximum flow rates of $\sim 43 \text{ Pa m}^3/\text{s}$ and a time between pulses of 1 s. The use of this gas pulsed mode was crucial for a controlled increase in the plasma density in ICRF discharge with simultaneous heating of plasma.

The time dependence of the line-averaged electron density was measured with a far-infrared (FIR) laser interferometer.²³ The temperature and electron density profiles were measured by the Thomson scattering (TS) system.²⁴ Time-resolved optical emission spectroscopy was used to detect the spectral lines of He I and H _{α} as well as from impurity ions (C III, C IV, O V, O VI, and Fe XVI). The total power radiated by plasma was measured with a bolometer.²⁵ To determine the gas composition and partial pressures, a quadrupole mass spectrometer system was enabled.

The plasma parameters time evolutions for a representative shot at the continuous mode of gas fueling are shown in Fig. 1. The discharge was initiated by the upper strap (U) of the HAS antenna. Then, with the delay of 700 ms, the FAIT (L) antenna was turned on. The plasma density increases slowly up to $\approx 1 \times 10^{19} \text{ m}^{-3}$ (see Fig. 2). The electron temperature ramps up faster, achieving its maximum of $\approx 1.3 \text{ keV}$ at the density value of $\approx 4.2 \times 10^{18} \text{ m}^{-3}$. Next, the density increases, and the temperature decreases and remains almost stationary at $\approx 1 \text{ keV}$. The maximum energy content of plasma in this shot was $\approx 0.05 \text{ MJ}$. At a maximum density value of $1.1 \times 10^{19} \text{ m}^{-3}$, the RF

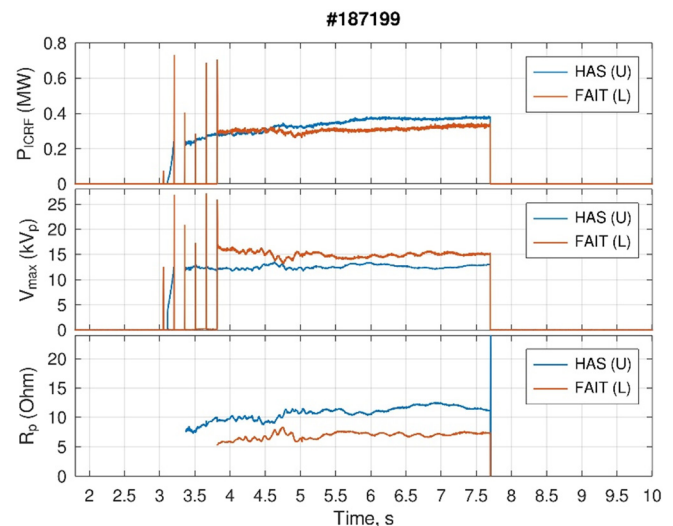


FIG. 1. Time evolutions of injection powers P_{ICRF} for antennas HAS (U), FAIT (L), maximum voltage at the coaxial line V_{max} , and loading resistances (including vacuum loading resistance) R_p for the LHD discharge #187199.

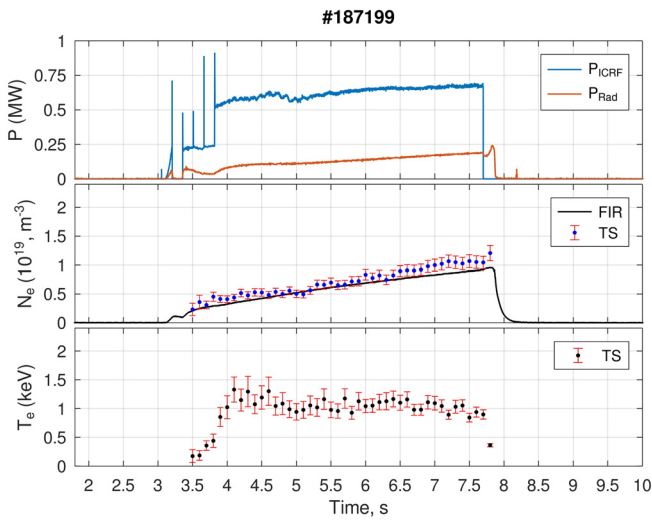


FIG. 2. Time evolutions of RF power P_{ICRF} (total), radiation power P_{Rad} , electron density N_e , and electron temperature T_e in continuous gas puff mode for the LHD discharge #187199. The average electron density of far-infrared (FIR) laser interferometer at $R = 3.669$ m, electron density, and temperature of Thomson scattering (TS) at $R = 3.602$ m are given. The initial working gas content is $\sim 30\%$ $H_2 + 70\%$ He.

power is ≈ 680 kW, with the radiation losses being not high, about ≈ 190 kW. After switching off the RF power at 7.7 s, the electron temperature decreases (see Fig. 2), while the density remains nearly unchanged. The plasma decay begins at ≈ 7.8 s.

This regime is very sensitive to the gas fueling rate. It does not depend strongly on the initial hydrogen concentration in the mixture, measured by mass spectrometry in the 16%–38% range.

Figure 3 shows the radial distribution of electron temperature and density for the discharge times 3.7 and 7 s. The temperature is

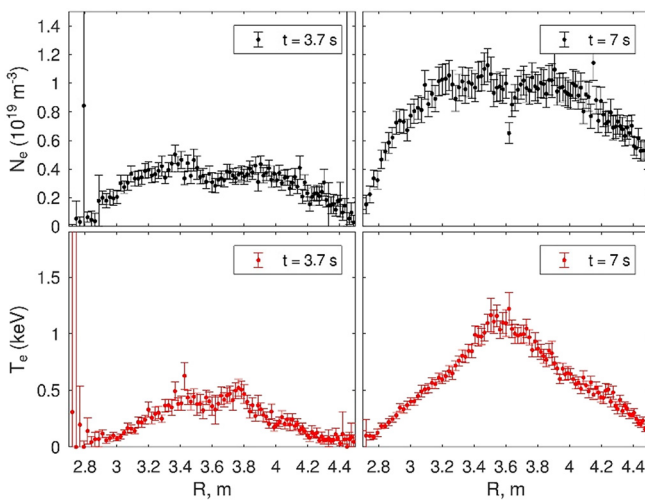


FIG. 3. Radial distribution of electron density and temperature (LHD discharge #187199) for $t = 3.7$ s (left panels) and 7.0 s (right panels).

maximum in the center of the plasma column, having triangular-shaped profile for $t = 7.0$ s, and somewhat flattened in the very center for $t = 3.7$ s. At the same time in 7 s, the electron density is roughly constant in the center of the profile ($R \sim 3.2\text{--}4$ m). Both the density and temperature of the electrons are about half for 3.7 s compared to 7 s.

Now, we turn to the new startup scheme. The salient feature of the scheme is pulsed gas injection. The HAS (U) antenna starts first, then, with a delay of 900 ms, the FAIT L and U parts antenna are powered (see Fig. 4). Helium gas pulses are applied from 3.5 to 7.5 s at a frequency of 1 Hz.

Figure 4 shows that the plasma density increases, and the electron temperature decreases after the first gas puff and an increase in the plasma density were observed after each gas injection pulse. Figure 4 also documents improved plasma conditions after the startup with the pulsed gas puff scheme: plasma densities around $0.8 \times 10^{19} \text{ m}^{-3}$, at an electron temperature of 2.5 keV, with an energy content of 0.1 MJ, and radiation losses up to 0.2 MW at 1.1 MW injected RF power were achieved. Figure 5 gives the RF system data for this shot.

Figure 6 shows waveforms of spectral lines in the startup phase. The shape of the intensity of the He I is a clear response to the gas puff pulse. In response to the first gas pulse, impurity ions Fe XVI, O V, O VI, and C IV lines are noticeably increased, indicating significant impurity release from the walls. Once additional RF power by the FAIT antenna is applied, however, all optical line intensities strongly decrease. The strong reduction of impurity lines goes along with a significant increase in the electron temperature. Thereafter, the intensities of the spectral lines of hydrogen and impurities do not change significantly, the impurity lines are much reduced, and all optical line intensities strongly decreased after switching on additional RF power by the

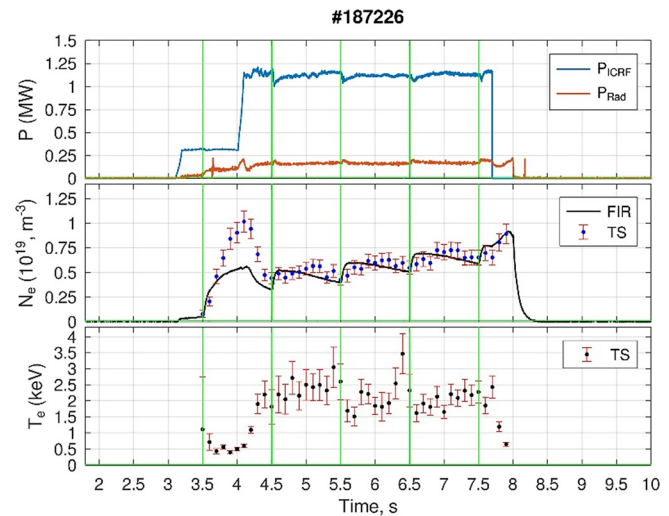


FIG. 4. Waveforms of the injected power P_{ICRF} (total), radiation power P_{Rad} , electron density N_e , and electron temperature T_e in with pulsed gas supply. The vertical green lines indicate gas puff moments. The data average electron density of far-infrared (FIR) laser interferometer at $R = 3.669$ m, electron density, and temperature of Thomson scattering (TS) at $R = 3.602$ m are given. The initial working gas content is $\sim 24\%$ $H_2 + 76\%$ He.

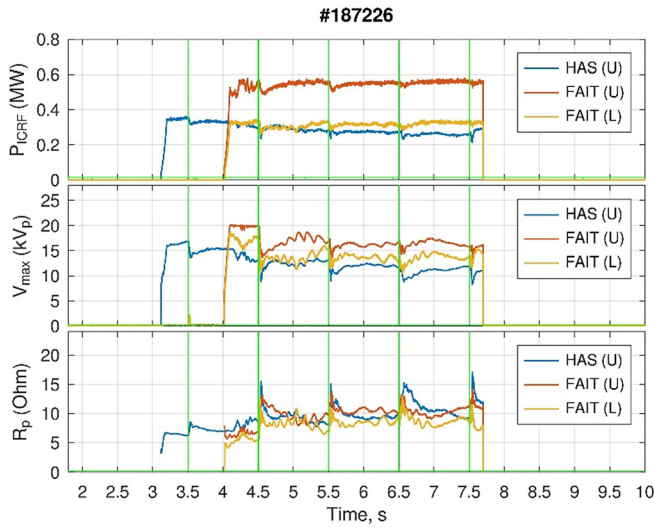


FIG. 5. Waveforms of injection ICRF power for antennas HAS (U), FAIT (U and L), maximum voltage at the coaxial line V_{max} , and loading resistances (including vacuum loading resistance) R_p for LHD discharge #187226. The vertical green lines indicate the times of gas puff pulses.

FAIT antenna. The initial concentration of hydrogen before the shot was $\sim 24\%$. During the RF, the hydrogen concentration can be estimated from the ratio of helium to hydrogen presented in Fig. 6. It can be seen that the hydrogen content decreases from pulse to pulse of helium injection. For example, before the second pulse, the ratio was ~ 0.5 , before the third pulse ~ 0.45 , and before the fifth pulse ~ 0.35 .

The radial distribution of the electron density and temperature is shown in Fig. 7. Similar shapes as for continuous gas supply appear

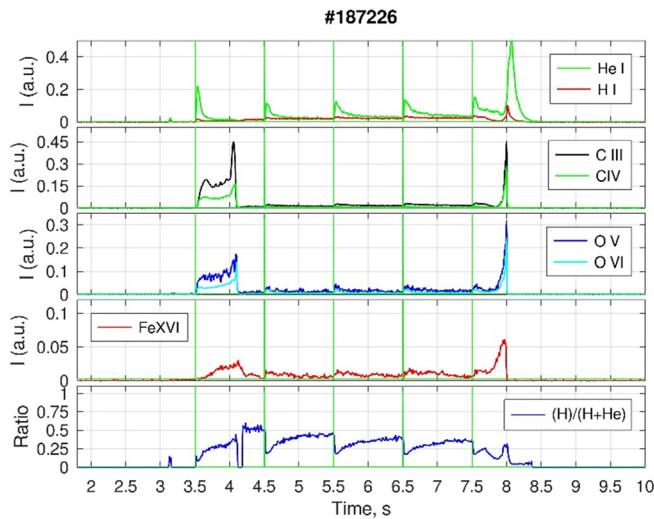


FIG. 6. Waveforms of spectral line intensities of H I (H_α 656.3 nm), He I (587.6 nm), and impurities C III (97.7 nm), C IV (154.9 nm), O V (63 nm), O VI (103.4 nm), and Fe XVI (33.5 nm), and percentage of hydrogen. The vertical green lines indicate gas puff.

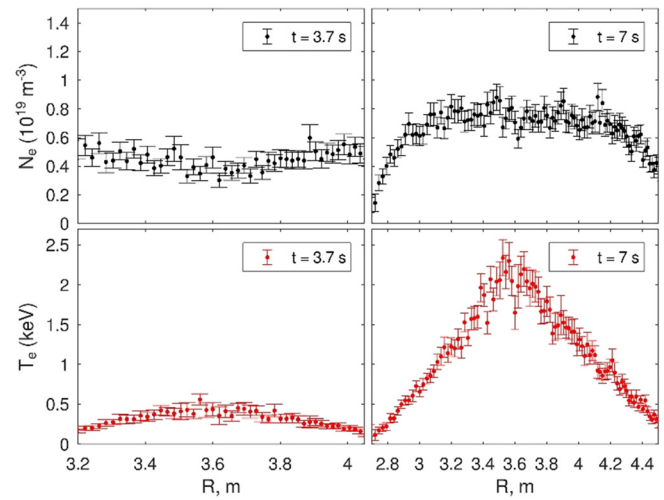


FIG. 7. Radial distribution of electron density and temperature (shot #187226) for times 3.7 and 7 s.

(Figs. 3 and 7) but at significantly enhanced electron temperatures. The elevated central electron temperature due to the increase in the ICRF power also shows a significant heating by ion cyclotron waves after the break-down phase.

Compared with previous experiments, in this study, the timing and amplitudes of the gas puff and the RF power were carefully tuned, and plasma production and heating were demonstrated for the first time only with exclusively ICRF heating in a big stellarator machine. In the regime with continuous gas puff, plasma density achieves the value of about $1 \times 10^{19} \text{ m}^{-3}$, and the electron temperature is over 1 keV. The ICRF power of 0.7 MW substantially exceeds the radiation power, 0.2 MW. For pulsed gas puff discharge, the ICRF power is higher, 1.1 MW. Radiation power and plasma density keep almost the same level. The electron temperature got higher values of 2–2.5 keV. As for electron-ion energy exchange, the estimated thermal equilibration time for electrons is 0.6 s. Therefore, energy losses for the Coulomb ion heating are not high. Both continuous and pulsed gas puffs could be employed to produce dense and hot plasmas. Target plasmas produced with the pulsed gas puff scheme show higher electron temperatures and are, therefore, better suited for a controlled increase in plasma density.

The significant increase in the central electron temperature beyond 1 keV is instrumental for target plasmas heated by the third cyclotron harmonics in the extraordinary mode (X3),²⁶ which requires high electron temperatures. Such a scenario is needed for Wendelstein 7-X for operation at a magnetic field of 1.7 T.²⁷ Moreover, plasmas with obtained parameters can be used as a target for neutral beam injection (NBI)²⁸ to provide target plasmas avoiding detrimental beam shine-through.

To conclude, the demonstrated startup scheme opens possibilities to develop different plasma production-heating scenarios in ICRF for stellarators that complement ECRH scenarios, significantly enhancing accessible plasma settings such as the magnetic field strength (given the fixed frequencies of resonance heating or the application of neutral beam injection). We point out two unique advantages: (i) ICRF startup does not have any upper plasma density limit, and (ii) for stellarators

having high magnetic fields, ICRF generators are available at an affordable price. Gyrotrons for X2 operation at high magnetic fields (potentially for reactor scale devices), however, are not yet developed.²⁹ For future improvements for ICRH plasma production, the extended experience accumulated on tokamaks (see, e.g., Refs. 30–32) will be useful.

This work has been carried out within the framework of the EUROfusion Consortium, funded by the European Union via the Euratom Research and Training Programme (Grant Agreement No. 101052200—EUROfusion). Views and opinions expressed are, however, those of the author(s) only and do not necessarily reflect those of the European Union or the European Commission. Neither the European Union nor the European Commission can be held responsible for them.

Useful discussions with Dr. J. Andersson along with a partial support from the Swedish Foundation for Strategic Research for one of the authors, V.E.M. (Grant No. UKR24-0015), are acknowledged.

We are pleased to acknowledge the assistance of the LHD Experiment Group.

The views and opinions expressed herein do not necessarily reflect those of the ITER Organization.

AUTHOR DECLARATIONS

Conflict of Interest

The authors have no conflicts to disclose.

Author Contributions

V. E. Moiseenko: Conceptualization (equal); Investigation (equal); Methodology (equal); Supervision (lead); Writing – original draft (equal); Writing – review & editing (equal). **Yu. V. Kovtun:** Conceptualization (equal); Formal analysis (equal); Investigation (lead); Methodology (equal); Validation (equal); Visualization (lead); Writing – original draft (lead); Writing – review & editing (equal). **H. Kasahara:** Data curation (equal); Investigation (equal); Methodology (equal); Writing – review & editing (equal). **T. Seki:** Data curation (equal); Investigation (equal); Methodology (equal); Writing – review & editing (equal). **K. Saito:** Investigation (equal). **R. Seki:** Investigation (equal). **S. Kamio:** Investigation (equal). **A. Dinklage:** Investigation (equal); Project administration (equal). **D. Hartmann:** Investigation (equal). **H. Laqua:** Investigation (equal). **T. Stange:** Investigation (equal). **S. Lazerson:** Investigation (equal). **A. Alonso:** Investigation (equal). **T. Wauters:** Investigation (equal). **Ye. O. Kazakov:** Investigation (equal). **J. Ongena:** Investigation (equal). **I. E. Garkusha:** Investigation (equal); Project administration (equal).

DATA AVAILABILITY

The data that support the findings of this study are openly available in LHD data at https://www-lhd.nifs.ac.jp/pub/Repository_en.html, Ref. 33.

REFERENCES

- T. Watari, “RF heating in stellarators,” *Plasma Phys. Controlled Fusion* **40**(8A), A13–A34 (1998).
- K. Nishimura, K. Matsuoka, M. Fujiwara, K. Yamazaki, J. Todoroki, T. Kamimura, T. Amano, H. Sanuki, S. Okamura, M. Hosokawa, H. Yamada, S.

- Tanahashi, S. Kubo, Y. Takita, and C. Takahashi, “Compact helical system physics and engineering design,” *Fusion Technol.* **17**(1), 86–100 (1990).
- W. Ballico, G. Cattanei, J.-M. Noterdaeme, W. Becker, F. Braun, F. Hofmeister, and F. Wesner, “Minority Heating Experiments on the W7-AS Stellarator,” *AIP Conf. Proc.* **244**(1), 150–154 (1992).
- V. E. Moiseenko, V. L. Berezhnyj, V. N. Bondarenko, P. Y. Burchenko, F. Castejón, V. V. Chechkin, V. Y. Chernyshenko, M. B. Dreval, I. E. Garkusha, G. P. Glazunov *et al.*, “RF plasma production and heating below ioncyclotron frequencies in Uragan torsatrons,” *Nucl. Fusion* **51**(8), 083036 (2011).
- V. E. Moiseenko, A. N. Shapoval, A. V. Lozin, V. V. Nemov, V. N. Kalyuzhnyi, M. M. Kozulya, R. O. Pavlichenko, V. G. Konovalov, A. E. Kulaga, Y. K. Mironov *et al.*, “Characteristics of regular discharges in Uragan-3M torsatron,” *Plasma Phys. Controlled Fusion* **61**(6), 065006 (2019).
- M. J. Hole, B. D. Blackwell, G. Bowden, M. Cole, A. Könies, C. Michael, F. Zhao, and S. R. Haskey, “Global Alfvén eigenmodes in the H-1 heliac,” *Plasma Phys. Controlled Fusion* **59**(12), 125007 (2017).
- Y. Torii, R. Kumazawa, T. Seki, T. Mutoh, T. Watari, K. Saito, T. Yamamoto, N. Takeuchi, Z. Cheng, Y. Zhao *et al.*, “Plasma production experiments using a folded waveguide antenna on LHD,” *Nucl. Fusion* **42**(6), 679 (2002).
- V. E. Moiseenko, Y. V. Kovtun, T. Wauters, A. Gorjaev, A. I. Lysoivan, A. V. Lozin, R. O. Pavlichenko, A. N. Shapoval, S. M. Maznichenko, V. B. Korovin *et al.*, “First experiments on ICRF discharge generation by a W7-X-like antenna in the Uragan-2M stellarator,” *J. Plasma Phys.* **86**(5), 905860517 (2020).
- M. Tripský, T. Wauters, A. Lysoivan, V. Bobkov, P. A. Schneider, I. Stepanov, D. Douai, D. Van Eester, J.-M. Noterdaeme, M. Van Schoor *et al.*, “A PIC-MCC code RFDinity1d for simulation of discharge initiation by ICRF antenna,” *Nucl. Fusion* **57**(12), 126043 (2017).
- R. Klima, A. V. Longinov, and K. N. Stepanov, “High-frequency heating of plasma with two ion species,” *Nucl. Fusion* **15**(6), 1157–1171 (1975).
- V. E. Moiseenko, Y. V. Kovtun, A. V. Lozin, R. O. Pavlichenko, A. N. Shapoval, L. I. Grigor’eva, M. M. Kozulya, S. M. Maznichenko, V. B. Korovin, E. D. Kramskoy *et al.*, “Plasma production in ICRF in the Uragan-2M stellarator in hydrogen–helium gas mixture,” *J. Fusion Energy* **41**, 15 (2022).
- Y. V. Kovtun, V. E. Moiseenko, A. V. Lozin, R. O. Pavlichenko, A. N. Shapoval, L. I. Grigor’eva, D. I. Baron, M. M. Kozulya, S. M. Maznichenko, V. B. Korovin *et al.*, “ICRF plasma production with the W7-X like antenna in the Uragan-2M stellarator,” *Plasma Fusion Res.* **17**, 2402034 (2022).
- Y. V. Kovtun, V. E. Moiseenko, A. V. Lozin, M. M. Kozulya, R. O. Pavlichenko, N. V. Zamanov, A. N. Shapoval, V. N. Bondarenko, D. I. Baron, S. M. Maznichenko *et al.*, “ICRF plasma production in gas mixtures in the Uragan-2M stellarator,” *Fusion Eng. Des.* **194**, 113887 (2023).
- Y. V. Kovtun, V. E. Moiseenko, S. Kamio, H. Kasahara, T. Seki, K. Saito, R. Seki, A. V. Lozin, R. O. Pavlichenko, A. N. Shapoval *et al.*, “ICRF plasma production with hydrogen minority heating in Uragan-2M and large helical device,” *Plasma Fusion Res.* **18**, 2402042 (2023).
- Y. V. Kovtun, V. E. Moiseenko, O. Lozin, M. Kozulya, R. Pavlichenko, A. Shapoval, V. Bondarenko, D. Baron, S. Maznichenko, V. Korovin *et al.*, “ICRF production of plasma with hydrogen minority in Uragan-2M stellarator by two-strap antenna,” *Phys. Plasmas* **31**(4), 042501 (2024).
- S. Kamio, V. E. Moiseenko, Y. Kovtun, H. Kasahara, K. Saito, R. Seki, M. Kanda, G. Nomura, T. Seki, Y. Takemura *et al.*, “First experiments on plasma production using field-aligned ICRF fast wave antennas in the large helical device,” *Nucl. Fusion* **61**(11), 114004 (2021).
- Y. V. Kovtun, H. Kasahara, V. E. Moiseenko, S. Kamio, T. Seki, K. Saito, R. Seki, A. Dinklage, D. Hartmann, H. Laqua *et al.*, “ICRF plasma production at hydrogen minority regime in LHD,” *Nucl. Fusion* **63**(10), 106002 (2023).
- V. E. Moiseenko, “ICRF plasma production and heating in LHD,” in *Proceedings of 29th IAEA Fusion Energy Conference* (IAEA, 2023), pp. 847–847.
- A. Iiyoshi, A. Komori, A. Ejiri, M. Emoto, H. Funaba, M. Goto, K. Ida, H. Idei, S. Inagaki, S. Kado *et al.*, “Overview of the large helical device project,” *Nucl. Fusion* **39**(9Y), 1245 (1999).
- H. Kasahara, K. Saito, T. Seki, R. Kumazawa, G. Nomura, F. Shimpo, S. Kubo, T. Shimozuma, H. Igami, T. Wakatsuki *et al.*, “The impact of ICRF heating using newly installed phasing antenna in LHD,” in *38th EPS Conference on Plasma Physics* (EPS, Strasbourg, 2011), Vol. 35G, p. P2.099.

- ²¹K. Saito, T. Seki, H. Kasahara, R. Seki, S. Kamio, G. Nomura, and T. Mutoh, "Field-aligned-impedance-transforming ICRF antenna in the LHD," *Fusion Eng. Des.* **96–97**, 583 (2015).
- ²²J. Miyazawa, K. Yasui, and H. Yamada, "Gas fueling system in LHD," *Fusion Eng. Des.* **83**, 265 (2008).
- ²³T. Akiyama, K. Kawahata, K. Tanaka, T. Tokuzawa, Y. Ito, S. Okajima, K. Nakayama, C. A. Michael, L. N. Vyacheslavov, A. Sanin *et al.*, "Interferometer systems on LHD," *Fusion Sci. Technol.* **58**(1), 352 (2010).
- ²⁴I. Yamada, H. Funaba, R. Yasuhara, H. Hayashi, N. Kenmochi, T. Minami, M. Yoshikawa, K. Ohta, J. H. Lee, and S. H. Lee, "Calibrations of the LHD Thomson scattering system," *Rev. Sci. Instrum.* **87**(11), 11E531 (2016).
- ²⁵B. J. Peterson, A. Y. Kostrioukov, N. Ashikawa, Y. Liu, Y. Xu, M. Osakabe, K. Y. Watanabe, T. Shimozuma, S. Sudo, and the LHD Experiment Group, "Bolometer diagnostics for one- and two-dimensional measurements of radiated power on the large helical device," *Plasma Phys. Controlled Fusion* **45**(7), 1167 (2003).
- ²⁶N. B. Marushchenko, P. Aleynikov, C. D. Beidler, A. Dinklage, J. Geiger, P. Helander, H. P. Laqua, H. Maassberg, Y. Turkin, and the W7-X Team, "Reduced field scenario with X3 heating in W7-X," *EPJ Web Conf.* **203**, 01006 (2019).
- ²⁷J. Ongena, D. Castano-Bardawil, K. Crombé, Y. O. Kazakov, B. Schweer, I. Stepanov, M. Van Schoor, M. Vervier, A. Krämer-Flecken, O. Neubauer *et al.*, "Physics design, construction and commissioning of the ICRH system for the stellarator Wendelstein 7-X," *Fusion Eng. Des.* **192**, 113627 (2023).
- ²⁸D. Gradic, A. Dinklage, R. Brakel, P. McNeely, M. Osakabe, N. Rust, R. Wolf, the W7-X Team and the LHD Experimental Group, "Assessment of the plasma start-up in Wendelstein 7-X with neutral beam injection," *Nucl. Fusion* **55**(3), 033002 (2015).
- ²⁹S. Karmakar and J. C. Mudiganti, "Gyrotron: The most suitable millimeter-wave source for heating of plasma in Tokamak," in *Plasma Science and Technology*, edited by A. Shahzad (IntechOpen, 2022).
- ³⁰Y. Kazakov, M. Nocente, M. J. Mantsinen, J. Ongena, Y. Baranov, T. Craciunescu, M. Dreval, R. Dumont, J. Eriksson, J. Garcia *et al.*, "Plasma heating and generation of energetic D ions with the 3-ion ICRF+ NBI scenario in mixed HD plasmas at JET-ILW," *Nucl. Fusion* **60**(11), 112013 (2020).
- ³¹P. Jacquet, P. Dumortier, E. Lerche, I. Monakhov, C. Noble, J. Roberts, H. Sheikh, A. Goodyear, N. Balshaw, D. Ciric *et al.*, "ICRH operations during the JET tritium and DTE2 campaigns," *Nucl. Fusion* **64**(6), 066039 (2024).
- ³²A. Cardinali, B. Baiocchi, C. Castaldo, R. Bilato, M. Brambilla, I. Casiraghi, S. Ceccuzzi, F. Napoli, G. L. Ravera, and A. A. Tuccillo, "Numerical investigation of the Ion Cyclotron Resonance Heating (ICRH) Physics in DTT," *J. Phys. Conf. Ser.* **2397**(1), 012017 (2022).
- ³³See https://www-lhd.nifs.ac.jp/pub/Repository_en.html for "LHD Experiment Data Repository."